Dynamic Scattering from Semiflexible Polymers

T. B. Liverpool*,† and A. C. Maggs

Physico-Chimie Theorique, ESA CNRS 7083, E.S.P.C.I., 75231 Paris Cedex 05, France

ABSTRACT: We study the dynamics and dynamic scattering functions of a semiflexible polymer of persistence length ℓ_p in the limit $q\ell_p \gg 1$, taking into account the *inextensibility* of the polymer chain *and* the effects of *hydrodynamics*. We find two distinct contributions to the scattering functions with different scaling behaviors in $q^2t^{3/4}$ and $q^2t^{7/8}$ coming from the *anisotropic* dynamics of the polymer. We also calculate the initial decay of the dynamic structure factor and obtain a novel t log t decay which allows us to explain recent dynamic light scattering experiments on viral particles.

Introduction

Quasi-elastic light scattering and inelastic neutron scattering have proven to be essential tools for studying the dynamics of polymeric systems. As a function of the scattering vector q and time, t, one can probe the internal modes of individual polymers or the large scale dynamics in polymer solutions. The theory of the dynamics and scattering of individual flexible polymers is now well understood.[1] If long-range hydrodynamic interactions are neglected (or are screened), the Rouse model shows that scattering functions can be expressed in a scaling form using the reduced variable $q^2t^{1/2}$. Hydrodynamics modifies this picture; however, one believes that a similar scaling picture is valid using the scaling variable $q^2t^{2/3}$.[2] The main aim of this paper is to discover how this picture is modified by the rigidity of the polymer. We perform calculations of the fluctuations and scattering functions of semiflexible polymer valid in the limit $q\ell_p \gg 1$, where ℓ_p is the persistence length of the polymer and q the scattering vector. We focus exclusively on time scales t short enough that the center of mass motion is negligible and bending modes of the polymer dominate the dynamics. In contrast with previous treatments of this problem, we find two competing contributions to the scattering functions which can be interpreted as being due to anisotropic fluctuations of the polymer in directions which are parallel to or perpendicular to the local orientation. We show that these two contributions can be studied and separated by either neutron scattering or by dynamic light scattering techniques on stiff polymers.

A number of theoretical approaches to the fluctuating dynamics of semiflexible polymers exist in the literature.[3−6] They all have a major defect in that they neglect the constraint of inextensibility in the dynamic equations, either by imposing the constraint "on average" at the very beginning of the calculation via a constant Lagrange multiplier[7] or by expansion about a linear reference state neglecting all constraints.[4,5] Similar remarks have already been made with respect to static correlations of stiff polymers.[8,9] These ad hoc approximations are sometimes successful, in particular in describing the intermediate time behavior of quasi-elastic light scattering data in stiff biopolymers.[4,10] In other situations, for instance the incoherent scattering function[6] or the initial slopes of the scattering function,[5] these approximations give an incorrect result as we shall show below.

Another approach current in the literature is to expand the contributions to the scattering functions as a series of dynamical normal modes.[11−13] While this gives a good description of the very long-time behavior when the dynamics is dominated by center of mass translation and rotation, it gives a poor account of the scattering functions at short and intermediate times. This is due to the fact that the truncation of the *infinite* sum of modes, while adequate for long times, breaks down at shorter times. The stretched exponential behavior we obtain in some regimes can be thought of as a compact resummation of these modes. An entirely analogous result is already known in the scattering from flexible polymers where the Zimm dynamic scattering function reduces to $g(\mathbf{q}, t) = g(\mathbf{q}, 0)e^{-\Gamma q^2 t^{2/3}}$ at intermediate times.[1,2] For very short times, the scattering function is analytic. For the longest times, the center of mass diffusion and rotations dominate the scattering.

In this paper, we perform a systematic expansion about a rod into longitudinal and transverse motion. The lowest or zeroth approximation is to ignore all the longitudinal motion and consider only the transverse dynamics.[4,5] A recent analytic treatment included the longitudinal motion[14] in a non-self-consistent manner. Subsequently, numerical work[15,16] showed that the mean square fluctuations of a stiff polymer have dynamical scaling that is highly anisotropic, characterized by two different sets of exponents for the parallel and perpendicular motion. Fluctuations perpendicular to the local axis of the polymer were found to scale as $\mathbf{r}_\perp^2 \sim t^{3/4}$ while fluctuations parallel to the local axis followed a surprisingly different law $\mathbf{r}_\parallel^2 \sim t^{7/8}$. In this paper, we show how to find this result *analytically* using a self-consistent treatment of the parallel and perpendicular dynamics. Using our results we reconsider recent DLS experiments on semiflexible viral particles. Detailed comparison[1] between experiments and older theories showed good, but not excellent agreement at longer times. At short times the agreement between experiments and theory is poor. The theory presented in this article shows that there are small but observable corrections in the longer time regime but that there are very significant modifications in the results for short time correlation functions which we are able to explicitly calculate.

The paper is organized as follows. In the next section, we review the equilibrium statistical mechanics of the wormlike chain emphasizing some subtleties having to do with inextensibility. In section III, we summarize

† Present address: Condensed Matter Theory Group, Blackett Laboratory, Imperial College, London SW7 2BZ, U.K.

10.1021/ma001468p CCC: $20.00
Published on Web 07/13/2001

dynamic light and neutron scattering from semiflexible polymer solutions. In section IV, we analyze the dynamics on length scales less than ℓ_p and calculate the two point transverse and longitudinal correlation functions. In section VI, we calculate the coherent structure factor. We analyze the different short and long time regimes. We calculate the incoherent structure factor in section V. Finally, we summarize our results in section VII making connection with experiments. In the more involved sections, we state the main results at the beginning of the section so that the reader only interested in the results need not get involved in the technical details of calculations.

II. The Model

The standard model of semiflexible polymers which we will study is the wormlike chain of Kratky and Porod[18] which takes into account the *bending* energy cost of the chain. We neglect the *twisting* energy of the polymer. This approximation and our justification for it is discussed in section IIB.

A. Dynamics of Wormlike Chains. The polymer conformation is parametrized by a curve $\mathbf{R}(s)$. The Hamiltonian of the wormlike chain is given by

$$\mathscr{H}_{\mathrm{wlc}}[\{\mathbf{R}(s)\}] = \frac{\kappa}{2}\int \mathrm{d}s\, [\partial_s{}^2\mathbf{R}]^2 \tag{1}$$

where in this and the following, for a function $A(x)$, $\partial_x A \equiv \partial A/\partial x$. The typical stretching energy of chain molecules is much higher than the bending energy and we may consider the chain as inextensible so that $|\partial_s\mathbf{R}|^2 = 1$. The persistence length is defined as $\ell_p = \kappa/k_BT$. We consider dilute solutions where interchain effects can be neglected.

We consider a wormlike chain of diameter a and persistence length $\ell_p \gg a$ parametrized as the space curve $\mathbf{R}(s)$. The polymer has total curvilinear length $L \gg a$. As discussed below we will restrict ourselves to length scales less than persistence length, $L < \ell_p$, as we can always consider a chain longer than the persistence length to be made up of "independent" sections shorter than ℓ_p. To study the equilibrium statistical mechanics we can begin with the partition function defined as

$$Z = \int \mathscr{D}[\mathbf{R}] \prod_s \delta[|\partial_s\mathbf{R}|^2 - 1] \exp(-\beta\mathscr{H}_{\mathrm{wlc}}) \tag{2}$$

The dynamics at finite T, i.e., taking into account the thermal fluctuations and Brownian motion, may be expressed by the Langevin equation[19]

$$\partial_t\mathbf{R}(s', t) = \int_0^L \mathrm{d}s\, \mathbf{H}[\mathbf{R}(s) - \mathbf{R}(s')]\cdot[-\kappa\partial_s{}^4\mathbf{R} + \tau(s, t)\partial_s{}^2\mathbf{R} + \partial_s\tau\partial_s\mathbf{R}] + \mathbf{V}(\{\mathbf{R}(s)\}, s, t) + \eta(\{\mathbf{R}(s)\}, s, t) \tag{3}$$

where $\tau(s, t)$ (a Lagrange multiplier) is an *instantaneous*, fluctuating "tension" which enforces the *local* inextensibility of the chain. We have defined $\mathbf{H}[\mathbf{r}]$, the mobility tensor which models the effect of hydrodynamics. The differentiability of $\mathbf{R}$ ensures the continuity of τ, i.e., the existence of $\partial_s\tau$. The inextensibility constraint fixes the tension, $\tau(s, t)$

$$0 = |\partial_s\mathbf{R}|^2 - 1 \tag{4}$$

The hydrodynamics generates a nondissipative term, $\mathbf{V}(\{\mathbf{R}(s)\}, s, t)$ and we have a Gaussian noise, $\eta(\{\mathbf{R}(s)\}, s, t)$. These are given respectively[20] by

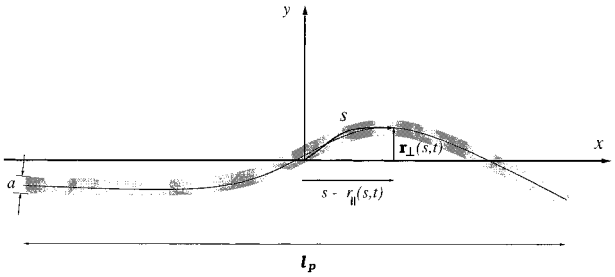

Figure 1. Transverse deformations of a wormlike chain on length scales less than ℓ_p oriented along the x-axis at time t so that $\mathbf{R}(s, t) = (s - r_\parallel(s, t), r_\perp(s, t))$ where we have defined the transverse, $r_\perp(s, t)$, and longitudinal, $r_\parallel(s, t)$, components of the motion.

$$V_i(\{\mathbf{R}(s)\}, s, t) = k_BT\int_0^L \mathrm{d}s'\nabla_j H_{ij}[\mathbf{R}(s) - \mathbf{R}(s')] \tag{5}$$

$$\langle\eta_i(\{\mathbf{R}(s)\}, s, t)\eta_j(\{\mathbf{R}(s')\}, s', t')\rangle = 2k_BTH_{ij}[\mathbf{R}(s) - \mathbf{R}(s')]\delta(t - t') \tag{6}$$

These equations describe the dynamics of an inextensible semiflexible polymer undergoing Brownian motion at finite T in the low Reynolds number hydrodynamic regime. We model the long-range hydrodynamics forces with the Oseen tensor[1]

$$\mathbf{H}[\mathbf{r}] = \frac{1}{8\pi\zeta_s|\mathbf{r}|}(\boldsymbol{I} + \hat{\mathbf{r}}\hat{\mathbf{r}}) \tag{7}$$

Of course, the Oseen description is only valid for $|\mathbf{r}| > a$. The viscosity of the solvent is given by ζ_s.

Sometimes, to good approximation, a local approximation to the friction is sufficient. In this case the mobility tensor is particularly simple $H_{ij}^{-1}(s - s') = \zeta_{ij}(s)\delta(s - s')$. We have purely local friction with an anisotropic friction matrix $\zeta(s)$ which is given by $\zeta(s) = \zeta_\perp^l(\mathbf{I} - \partial_s\mathbf{R}\partial_s\mathbf{R}) + \zeta_\parallel^l\partial_s\mathbf{R}\partial_s\mathbf{R}$ where $\zeta_\perp^l$ and $\zeta_\parallel^l$ are the perpendicular and parallel *local* friction coefficients respectively given by $\zeta_\parallel^l = 2\pi\zeta_s = {}^1/_2\zeta_\perp^l$. As we shall see later, while this local approximation is good for capturing the long-time behavior of the wormlike chain, it fails when one considers the short-time behavior.

Unfortunately, the dynamical equations (eqs 3 and 4) above are terribly nonlinear and cannot be solved exactly. Progress can only be made in some special limits, a particular one being the *rodlike* regime where we can make a *systematic* perturbation around a rod. A schematic is shown in Figure 1. We, without loss of generality, orient the rod along the x axis and write

$$\mathbf{R}(s) = (s - r_\parallel, \mathbf{r}_\perp) \tag{8}$$

where $r_\parallel, |\mathbf{r}_\perp| \ll s$ so that we can perform a small gradient expansion, e.g., $\partial_s\mathbf{R} = (1 - \partial_s r_\parallel, \mathbf{r}_\perp) \simeq (1, 0) + O(\partial_s\mathbf{r}_\perp)$. We have a longitudinal (along the rod axis, $\parallel$) and a transverse (perpendicular to the rod axis, $\perp$) component. These two motions are not independent, since they can be linked by the incompressibility of the filament as first stated clearly by Gittes et al.[14] It is important to note that $r_\parallel(s)$ is the *difference* between the longitudinal component and s, the value it would have for a "perfect" rod. The complete longitudinal component is $s - r_\parallel$ and *not* $r_\parallel$ where $s \gg r_\parallel$. We emphasize that by making an

expansion about a rod and implementing the inextensibility constraint, *exactly* the end-to-end distribution we would calculate is *not* Gaussian[9] but rather strongly peaked about a rod.

B. The Torsional Modes. The above discussion of a polymer in terms of an inextensible fluctuating filament with only a bending energy contains an important simplification compared with true stiff polymers: the neglect of the torsional degrees of freedom. In this section, we briefly summarize the justification for this simplification, adding some remarks as to when this could break down.

In general the torsional dynamics and bending dynamics are coupled via the writhe.[21] Indeed it is understood that a torsional excitation can relax via either spinning motion about the polymer axis at constant polymer shape, the so-called "speedometer dynamics",[22] or via crankshaft motion which strongly couples twist and bend dynamics. It has been argued using scaling arguments[23,24] that crankshaft motion presents a much higher friction coefficient to relaxation so that the dominant dynamics in a torsionally rigid, stiff polymer can be considered as being "tubelike" That is the torsional modes relax rapidly and easily at constant shape just as they could do if confined by a confining gel. The bending modes then slowly modify the tube position. These rather subtle ideas have been verified numerically by Maggs:[25] in simulations of a stiff, torsionally rigid polymer, it was found that the torsional motion gave rise to no crankshaft motion even for polymers which had a length of many times the persistence length. We have also used the same simulation code to verify that the power law behaviors found in the present article for the longitudinal and transverse motion, which couple to density fluctuations and hence scatter light are not modified by the coupling between torsion and bending in the scaling regimes that are considered in this paper. We are thus justified in neglecting this coupling for our calculations in stiff straight polymers. The quality of this approximation increases with the ratio of the persistence length to polymer diameter. While small deviations from the theory presented here may be present for moderately stiff molecules, such as DNA, the deviations should be negligible in stiffer filamentary systems such as actin.

We note that in DNA the situation can be even more delicate.[26] Fluctuations in local chemical composition imply that the zero temperature center line is not straight. This can increase the strength of torsional-bend coupling. In the case of strongly driven twisting of DNA (that for example occurs during replication) this can lead to enhanced buckling and rotational drag.[23] We shall leave open the question of the effect of this coupling on the thermally driven bending and twisting considered in this paper. Clearly a DNA sequence containing many bend sequences cannot be understood with a theory based on a straight ground state; the result of scattering from DNA molecules could thus contain an important dependence on base sequence.

III. Light and Neutron Scattering

In this section, we remind the reader of a number of standard results on the scattering of radiation from polymeric systems.[27] This allows us to introduce the notation used for the rest of the paper. We define the scattering cross-section σ_s as the total number of neutrons (photons) scattered per second divided by the intensity of the incident beam. For radiation of incident momentum $\mathbf{k_i}$ and final momentum $\mathbf{k_f}$ we define a scattering wave vector $\mathbf{q} = \mathbf{k_i} - \mathbf{k_f}$. The differential cross-section at a *scattering* wave vector $\mathbf{q}$ of a sample of N scatterer at positions $\mathbf{r}_i$ where $1 \le i \le N$ is the cross-section scattered at a solid angle Ω and at frequency ω

$$\frac{d^2\sigma_s}{d\Omega\, d\omega}(\mathbf{q},\omega) = \frac{k_f}{k_i}\frac{1}{2\pi}\sum_{i,j}^{N} b_i b_j \int_{\infty}^{-\infty} \exp(i\omega t)\, dt \times \langle \exp[-i\mathbf{q}\cdot(\mathbf{r}_i(t) - \mathbf{r}_j(0))]\rangle \quad (9)$$

where b_i is the scattering length of scatterer i.

Defining a "mean" scattering length $b = \langle b\rangle \equiv (1/N)\sum_j b_j$ and its variance, $(\Delta b)^2 = \langle b^2\rangle - \langle b\rangle^2$, we can rewrite the scattering cross-section as

$$\frac{d^2\sigma_s}{d\Omega\, d\omega}(\mathbf{q},\omega) = \frac{N}{2\pi}\frac{k_f}{k_i}\{(\Delta b)^2 S_{inc}(\mathbf{q},\omega) + b^2 S_{coh}(\mathbf{q},\omega)\} \quad (10)$$

where we have defined the *incoherent* structure function, $S_{inc}(\mathbf{q},\omega)$, which probes the motion of individual scattering centers and the *coherent* structure function, $S_{coh}(\mathbf{q},\omega)$ which probes the motion of the ensemble of molecules. Labeling techniques enable one to measure the two contributions independently in neutron scattering. In light scattering, one usually measures the coherent scattering function, but use of strongly scattering microbeads[1] should also allow one to have access to the incoherent function in light scattering as well.

For an isolated polymer with N monomers of size a of total length $L = Na$, we obtain the *incoherent* structure function:

$$S_{inc}(\mathbf{q}, t) \equiv \int_{\infty}^{-\infty} \exp(-i\omega t)\, d\omega\; S_{inc}(\mathbf{q},\omega) = \frac{1}{N}\int_0^L \frac{ds}{a} \langle \exp[i\mathbf{q}\cdot(\mathbf{R}(s, t) - \mathbf{R}(s, 0))]\rangle \quad (11)$$

Similarly we find the *coherent* structure function:

$$S_{coh}(\mathbf{q}, t) = \frac{1}{2N}\int_0^L \frac{ds}{a}\int_0^L \frac{ds'}{a} \langle \exp[i\mathbf{q}\cdot(\mathbf{R}(s, t) - \mathbf{R}(s', 0))]\rangle \quad (12)$$

Reiterating the discussion at the end of the previous section, see eq 8, we can split the chain into sections of length less than ℓ_p. For each section it is useful to split the chain position into perpendicular and parallel components to a given orientation. For a section of chain with a given orientation we can write $\mathbf{q} = (q_{\|},\mathbf{q}_\perp)$ where $q_{\|} = q\cos\theta$ and $|\mathbf{q}_\perp| = q\sin\theta$. We perform averages over the transverse and longitudinal fluctuations and obtain the orientation-dependent structure function.

$$S_{inc}(\theta,\mathbf{q}, t) = \frac{1}{N}\int \frac{ds}{a} \exp\left[-\frac{q_\perp^2}{4}\langle(\mathbf{r}_\perp(s, t) - \mathbf{r}_\perp(s, 0))^2\rangle - \frac{q_{\|}^2}{4}\langle(r_{\|}(s, t) - r_{\|}(s, 0))^2\rangle\right] \quad (13)$$

Finally for an isotropic chain distribution we average over orientations to get

$$S_{\rm inc}(\mathbf{q}, t) = \frac{1}{2}\int_{-1}^{1} {\rm d}(\cos\theta) S_{\rm inc}(\theta, \mathbf{q}, t) \qquad (14)$$

This may be evaluated easily

$$S_{\rm inc}(\mathbf{q}, t) = \frac{1}{2}\int_{-1}^{1} {\rm d}x \exp\left[-\frac{q^2}{4}(x^2 J_{\|}(0, t) + (1 - x^2) J_{\perp}(0, t))\right] \qquad (15)$$

where $x = \cos\theta$ and we have defined the *transverse* and *longitudinal* two-time connected correlation functions $J_\perp$ and $J_{\|}$ respectively

$$J_{\perp}(s - s', t - t') \equiv \langle [\mathbf{r}_{\perp}(s, t) - \mathbf{r}_{\perp}(s', t')]^2 - [\mathbf{r}_{\perp}(s, t') - \mathbf{r}_{\perp}(s', t')]^2 \rangle \qquad (16)$$

and

$$J_{\|}(s - s', t - t') = \langle [r_{\|}(s, t) - r_{\|}(s', t')]^2 - [r_{\|}(s, t') - r_{\|}(s', t')]^2 \rangle \qquad (17)$$

Doing the same thing for the coherent structure function and after the average over orientations, we obtain

$$S_{\rm coh}(\mathbf{q}, t) = \frac{1}{4N}\int_{-1}^{1} dx \int \frac{{\rm d}s}{a} \int \frac{{\rm d}s'}{a} \exp[iqx(s - s')] \times \exp\left[-\frac{q^2(1 - x^2)}{4} K_{\perp}(s - s', t) - \frac{q^2 x^2}{4} K_{\|}(s - s', t)\right] \qquad (18)$$

where we have defined the complete dynamic correlation functions

$$K_{\perp}(s, t) = \langle (\mathbf{r}_{\perp}(s, t) - \mathbf{r}_{\perp}(0, 0))^2 \rangle \qquad (19)$$

and

$$K_{\|}(s, t) = \langle (r_{\|}(s, t) - r_{\|}(0, 0))^2 \rangle \qquad (20)$$

which we can write in terms of a static part $K_i^{(0)}(s) = K_i(s, 0)$ and and a dynamic part $J_i(s, t)$, $K_i(s, t) = J_i(s, t) + K_i(s, 0) \equiv J_i(s, t) + K_i^{(0)}(s)$ where $\{i\}$ refers to $\{\|,\perp\}$. The static correlation functions are given by[4] $K_\perp^{(0)}(s) \sim s^2 L/\ell_{\rm p}$ and $K_{\|}^{(0)}(s) \sim s^2 L^2/\ell_{\rm p}^2$.

IV. Transverse and Longitudinal Dynamics

A. Summary of Section Results. As found by previous authors,[4,5] our analysis of the transverse dynamics finds that the transverse fluctuations are correlated over a length, $\ell_\perp(t)$, of the chain

$$\ell_{\perp}(t) = \left(\frac{t\ell_{\rm p} k_{\rm B} T}{\zeta_{\perp}}\right)^{1/4} \qquad (21)$$

where the transverse friction coefficient $\zeta_\perp = 4\pi\zeta_{\rm s}$ and $\zeta_{\rm s}$ is the viscosity of the solvent (water). In particular, we calculate the two-time transverse correlation functions defined in the previous section, see eq 16, as

$$J_{\perp}(s, t) = \frac{8(\ell_{\perp}(t))^3}{\pi\ell_{\rm p}} \int_{\ell_\perp/L \to 0}^{\ell_\perp/a} dz \left\{\frac{1}{z^4}(1 - {\rm e}^{-z^4(|\log A_{\perp}(z,t)| - \gamma)}) \times \cos\left(A_{\perp}(z,t)\frac{s}{a}\right)\right\} \sim t^{3/4} f_{\perp}\left(\frac{s}{t^{1/4}}\right) \qquad (22)$$

$$J_{\perp}(0, t) \simeq \frac{8\Gamma(^1/_4)}{3\ell_{\rm p}\pi}(\ell_{\perp}(t))^3(\log[\ell_{\perp}(t)/a])^{3/4} \sim t^{3/4} \qquad (23)$$

where $A_\perp(z, t) = za/\ell_\perp(t)$. The Euler γ constant is given by $\gamma \simeq 0.5772$ and $f_\perp(x) \sim \int_0^\infty {\rm d}z \cos(zx)(1 - {\rm e}^{-z^4})/z^4$. This expression is valid for time scales $t > t_{\rm min}$; where $\ell_\perp(t_{\rm min}) \sim a$ is below those time scales, the mode dynamics of the polymer's internal structure dominate. Since we are concerned with the dynamics of the bending modes, we have ignored end effects. Therefore, it is also essential that $t < t_{\rm max}$ where $\ell_\perp(t_{\rm max}) \sim L$. For $t > t_{\rm max}$, all the *local* transverse fluctuations we would have propagated to the ends of the polymer and be fully *relaxed* so that $J_\perp(s, t > t_{\rm max}) = 0$.

In contrast to the transverse case, we find that the longitudinal fluctuations are correlated over a *different* length $\ell_{\|}(t)$ given by

$$\ell_{\|}(t) = (t\ell_\vartheta^5 k_{\rm B} T/\zeta_{|})^{1/8} \qquad (24)$$

where the longitudinal friction coefficient $\zeta_{\|} = 2\pi\zeta_{\rm s}$ and we have defined an intermediate length of the order of the persistence length $\ell_\vartheta = \ell_{\rm p} 2^{7/5}(\zeta_\perp/\zeta_{\|})^{3/5}$.

We find that the two-time longitudinal fluctuation defined in eq 17 is given by

$$J_{\|}(s, t) = \frac{8(\ell_{\|}(t))^7}{\ell_\vartheta^5 \pi} \int_{\ell_\|/L \to 0}^{\ell_\|/a} dz \left\{\frac{1}{z^8(|\log A_{\|}(z, t)| - \gamma)^3} \times (1 - {\rm e}^{-z^8(|\log A_{\|}(z,t)| - \gamma)^4}) \cos\left(A_{\|}(z, t)\frac{s}{a}\right)\right\} \sim t^{7/8} f_{\|}\left(\frac{s}{t^{1/8}}\right) \qquad (25)$$

$$J_{\|}(0, t) \simeq \frac{8\Gamma(^1/_8)}{7(2\ell_{\rm p})^5\pi}(\ell_{\|}(t))^7(\log[\ell_{\|}(t)/a])^{1/2} \sim t^{7/8} \qquad (26)$$

where $A_\|(z, t) = za/\ell_\|(t)$ and $f_\|(x) \sim \int_0^\infty {\rm d}z \cos(zx)(1 - {\rm e}^{-z^8})/z^8$. Note that for long stiff polymers $\zeta_\perp = 2\zeta_\|$ so that $\ell_\vartheta = 2\ell_{\rm p}$. We stress again that we have ignored end effects and we are not interested in the "internal" structural modes of the polymer. Therefore, this expression is valid for t such that $L \gg \ell_\|(t) \gg a$.

Our expressions for $J_\perp$ and $J_\|$ are in agreement with recent numerical results on the anisotropic dynamics of semiflexible polymers.[15] In particular, the time dependence of these two quantities is very different, as are the spatial correlations, characterized by $\ell_\| \sim t^{1/8}$ and $\ell_\perp \sim t^{1/4}$.

B. Small Gradient Expansion. Taking account of the long-range hydrodynamics by using the Oseen tensor and using eqs 3 and 8, we decompose the Langevin equation into its $\perp$ and $\|$ components. For small gradients ($|\partial_{\rm s}\mathbf{r}_\perp| \ll 1$), we can make a *systematic* expansion in $\partial_{\rm s}\mathbf{r}_\perp$ keeping all terms up to $O(|\partial_{\rm s}\mathbf{r}_\perp|^2)$ (i.e., the lowest order nonlinearities). The Langevin equation of motion becomes

$$\partial_t \mathbf{r}_\perp(s,t) = 1/\zeta_\perp \int ds' \frac{1}{|s-s'|}[-\kappa \partial^4_{s'} \mathbf{r}_\perp + \tau(s',t)^2 \partial_{s'} \mathbf{r}_\perp + \partial_{s'} \tau \partial_{s'} \mathbf{r}_\perp] + \eta_\perp(s,t) + O(|\partial_s \mathbf{r}_\perp|^3) \quad (27)$$

$$\partial_t r_{||}(s,t) = \frac{1}{\zeta_{||}} \int ds' \frac{1}{|s-s'|}[-\kappa \partial_{s'}{}^4 r_{||} - \partial_{s'} \tau] + \eta_{||}(s,t) + O(|\partial_s \mathbf{r}_\perp|^3) \quad (28)$$

where $\zeta_{||} = 2\pi\zeta_s = {}^1/_2\zeta_\perp$ and $\eta = (\eta_{||}, \eta_\perp)$.

Using eqs 4 and 8, we find that the inextensibility constraint $\partial_s r_{||} = {}^1/_2 |\partial_s \mathbf{r}_\perp|^2 (1 - \partial_s r_{||})^{-1}$ can be written for $\partial_s r_{||} \ll 1$ as

$$\partial_s r_{||} = \frac{1}{2} |\partial_s \mathbf{r}_\perp|^2 + O(|\partial_s \mathbf{r}_\perp|^4) \quad (29)$$

The noise has zero mean, $\langle \eta(s,t) \rangle = 0$, and mean square fluctuations

$$\langle \eta_i(s,t) \eta_j(s',t') \rangle = 2k_B T \delta_{ij} \frac{1}{\zeta_i |s-s'|} \delta(t-t') \quad (30)$$

where the subscripts $\{i\}$ refer to || or $\perp$.

The coupled eqs 27−29 and the noise correlations, eq 30, contain the dynamics of the semiflexible polymer for length scales less than ℓ_p which we proceed to solve self-consistently. This is done by using eq 29 to link the two nonlinear eqs 27 and 28 and to generate a linear equation for $r_{||}$. If we ignore the long range hydrodynamic forces and consider only a local friction, we replace $|s-s'|^{-1}$ by $\delta(s-s')$ in eqs 27 and 28 and replace ζ_i by ζ_i^l, the anisotropic friction of a rod in a viscous fluid.

We find it convenient to go to frequency−momentum space. We are studying the dynamics on length scales much less than the length of the polymer and so are interested in properties independent of the boundary conditions at the ends of the polymer. Therefore, we extend the s integrals to infinity and perform Fourier transforms, $\mathbf{r}_\perp(s,t) = \int (dq/2\pi)(dq/2\pi) \mathbf{r}_\perp(q,\omega) \exp[i(qs + \omega t)]$. We have a short-distance cutoff which is set by the polymer diameter, $|s-s'| > a$.

In frequency-momentum space, eq 27 can be written

$$i\omega \mathbf{r}_\perp(q,\omega) = \mathbf{H}_\perp(q)\left(-\kappa q^4 \mathbf{r}_\perp(q,\omega) - q \int \frac{dk}{2\pi} \frac{d\Omega}{2\pi} k\tau(q-k, \omega-\Omega) \mathbf{r}_\perp(k,\Omega)\right) + \eta_\perp(q,\omega) \quad (31)$$

where

$$\mathbf{H}_\perp(q) = \frac{1}{(8\pi\zeta_s a)} \int_a^\infty ds \frac{2\cos qs}{s} = -\frac{1}{\zeta_\perp}(\log qa + \gamma) + O(q^2) \quad (32)$$

is the Fourier transform of the transverse part of the Oseen tensor. We can rewrite eq 31 as

$$\mathbf{r}_\perp(q,\omega) = G_0(q,\omega)\eta_\perp(q,\omega) + \frac{q(\log qa + \gamma)}{\zeta_\perp} G_0(q,\omega) \int \frac{dk}{2\pi} \frac{d\Omega}{2\pi} k\tau(q-k, \omega-\Omega) \mathbf{r}_\perp(k,\Omega) \quad (33)$$

where we have defined a zeroth order response function

$$G_0(q,\omega) \equiv \frac{1}{i\omega - \alpha q^4 (\log qa + \gamma)} \quad (34)$$

The constant α is defined as $\alpha \equiv \kappa/\zeta_\perp$. The noise fluctuations are given by

$$\langle \eta_i(q,\omega) \eta_j(q',\omega') \rangle = 2k_B T \delta_{ij} \frac{(2\pi)^2}{\zeta_i} (-\log qa - \gamma) \delta(q+q') \delta(\omega+\omega') \quad (35)$$

To keep our formulas compact, we omit the Euler constant in the calculations which follow. As the $\log ka$ dominates the γ for small k, this is a very reasonable approximation. For completeness, we have re-included it in the final expressions, eqs 22 and 25. Since $\langle \tau(s,t) \rangle = 0$, we can calculate the leading part of the transverse dynamics with G_0 (remembering that there are two independent modes); setting $\tau = 0$, we calculate the transverse correlation function (see eq 16)

$$J_\perp(s,t) = \frac{8k_B T}{\zeta_\perp} \int\int \frac{dq}{2\pi} \frac{d\omega}{2\pi} |\log qa| G_0(q,\omega) G_0(-q,-\omega)(\cos(qs) - \cos(qs + \omega t)) \quad (36)$$

which gives eq 22.

C. Self-Consistent Calculation. We can perform a self-consistent calculation of the coupled eqs 27−29. Returning to eq 27, using the operator formalism, we define an operator $G_0^{-1} = \partial_t + \mathbf{H} \cdot \alpha \partial_s^4$, where $\mathbf{H}$ is the Oseen tensor and $\alpha = \kappa/\zeta_\perp$, and we can write eq 27 formally as

$$\mathbf{r}_\perp = (G_0 \eta_\perp + G_0 \Sigma(s) \mathbf{r}_\perp) \quad (37)$$

where we have defined the operator, $\Sigma(s) = \mathbf{H} \cdot (\tau \partial^2_s + \partial_s \tau \partial_s)$, and obtain the result as an expansion in Σ (or τ)

$$\mathbf{r}_\perp = (\mathbf{I} - G_0\Sigma)^{-1} G_0 \eta_\perp = G_0\eta_\perp + (G_0\Sigma) G_0 \eta_\perp + O(\Sigma^2) \quad (38)$$

Using eq 38, we calculate the rhs of the constraint of chain inextensibility, eq 29, as

$$\frac{1}{2}|\partial_s \mathbf{r}_\perp|^2 = \frac{1}{2}|(\mathbf{I} - G_0\Sigma)^{-1} \partial_s (G_0\eta_\perp) + (\mathbf{I} - G_0\Sigma)^{-2} \partial_s (G_0\Sigma) G_0 \eta_\perp|^2 \quad (39)$$

leading to an expression for eq 29 as an expansion in Σ

$$2\partial_s r_{||} = |\partial_s (G_0\eta_\perp)|^2 + 2|\partial_s (G_0\eta_\perp)|^2 G_0 \Sigma + 2\partial_s (G_0\eta_\perp) \partial_s (G_0\Sigma) G_0 \eta_\perp + O(\Sigma^2) \quad (40)$$

We now perform averages over the transverse noise, $\eta_\perp$. After performing the *transverse* noise averages and integrating by parts, eq 40 gives a nonlinear relationship between $r_{||}$ and τ *due* to the *transverse* motion, as a series in τ i.e., $2\partial_s r_{||} = 2\partial_s r_{||}^{(0)} + \mathbf{R} \cdot \Sigma + O(\Sigma^2)$ where $\partial_s r_{||}^{(0)}$ is the equilibrium value and $\mathbf{R} = -\langle 2\partial_s^2 (G_0\eta_\perp) - G_0 G_0 \eta_\perp \rangle$ an operator. But we also have the "exact" (for small gradients) dynamical eq 28 showing the relationship between the $r_{||}$ dynamics and τ. We consistently sum all the contributions from the dynamics of $\mathbf{r}_\perp$ to the $r_{||}$ dynamics by substituting the leading (linear) term of eq 40 into eq 28. In other words, the self-consistent

calculation corresponds to a re-summation of all the diagrams to all orders in τ of the inextensibility constraint using the dissipative longitudinal dynamics. A diagrammatic representation of eq 40 is shown in Figure 2.

The self-consistent calculation can be understood in another way. First, we have used the incompressibility constraint *and* the dynamics of the transverse modes to self-consistently calculate the tension as a linear function of the longitudinal motion. Second, from the dynamical equation for $r_{||}$, eq 28, the longitudinal dynamics is driven by tension gradients. Therefore, we eliminate τ in the dynamical eq 28 for the $r_{||}$ to get a *linear* Langevin equation in $r_{||}$.

We now put our formal discussion above into concrete calculations. Explicitly we perform an expansion in τ so that eq 31 for $\mathbf{r}_\perp$ may be solved iteratively (see eq 38). We have one $\tau - \mathbf{r}_\perp$vertex. We expand to linear order in τ

$$\mathbf{r}_\perp(q,\omega) = G_0(q,\omega)\eta_\perp(q,\omega) - \frac{1}{\zeta_\perp}G_0(q,\omega)q|\log qa| \times \int \frac{\mathrm{d}k}{2\pi}\frac{\mathrm{d}\Omega}{2\pi} k\tau(q-k,\omega-\Omega)G_0(k,\Omega)\eta_\perp(k,\Omega) + O(\tau^2) \tag{41}$$

The inextensibility constraint becomes

$$iqr_{||}(q,\omega) = -\frac{1}{2}\int \frac{\mathrm{d}k}{2\pi}\frac{\mathrm{d}\Omega}{2\pi} k(q-k)\mathbf{r}_\perp(k,\Omega)\cdot\mathbf{r}_\perp(q-k,\omega-\Omega) \tag{42}$$

Using eq 41, this may be evaluated to $O(\tau^2)$ as

$$iqr_{||}(q,\omega) = -\frac{1}{2}\int \frac{\mathrm{d}k}{2\pi}\frac{\mathrm{d}\Omega}{2\pi} k(q-k) \times \Bigg[G_0(k,\Omega)G_0(q-k,\omega-\Omega)\eta_\perp(k,\Omega)\cdot\eta_\perp(q-k,\omega-\Omega) - \frac{\log ka}{\zeta_\perp}G_0(q-k,\omega-\Omega) \times \eta_\perp(q-k,\omega-\Omega)\cdot G_0(k,\Omega)\int \frac{\mathrm{d}p}{2\pi}\frac{d\chi}{2\pi} \times kp\tau(k-p,\Omega-\chi)G_0(p,\chi)\eta_\perp(p,\chi) - \frac{\log|(q-k)a|}{\zeta_\perp} \times G_0(k,\Omega)\eta_\perp(k,\Omega)\cdot G_0(q-k,\omega-\Omega) \times \int \frac{\mathrm{d}p}{2\pi}\frac{d\chi}{2\pi}(q-k)p\tau(q-k-p,\omega-\Omega-\chi) \times G_0(p,\chi)\eta_\perp(p,\chi)\Bigg] + O(\tau^2) \tag{43}$$

We now perform an average over the transverse modes to obtain finally

$$iqr_{||}(q,\omega) = -\tau(q,\omega)R(q,\omega) + \langle iqr_{||}(q,\omega)\rangle_\perp \tag{44}$$

where $\langle\cdots\rangle_\perp$ represents an average over the transverse modes $\langle iqr_{||}(q,\omega)\rangle_\perp = ((2\pi)^2/\zeta_\perp)4k_BT\delta(q)\delta(\omega)\int(\mathrm{d}k/2\pi)(\mathrm{d}\Omega/2\pi)k^2(\log ka + \gamma)[G_0(k,-\Omega)]^2$ and

$$R(q,\omega) = \frac{2k_BT}{\zeta_\perp{}^2}\int \frac{\mathrm{d}k}{2\pi}\frac{\mathrm{d}\Omega}{2\pi} k^2(q-k)^2\log ka \log|(q-k)a| \times [G_0(k,-\Omega)G_0(k,\Omega)G_0(q-k,\Omega-\omega) + G_0(q-k,\Omega-\omega)G_0(q-k,\omega-\Omega)G_0(k,-\Omega)] \tag{45}$$

We evaluate $R(q,\omega)$ for $q^4 \ll |\omega|/\alpha$. There are two main reasons for this. First, we are looking for the contribution to the tension from the transverse dynamics (we need to look at longer wavelength than the modes which we are summing over). Second, the wavelengths $q^4 \gg |\omega|/\alpha \sim |\omega|\zeta_{||}/\kappa$ will be dominated by the bending contribution to the longitudinal dynamics.

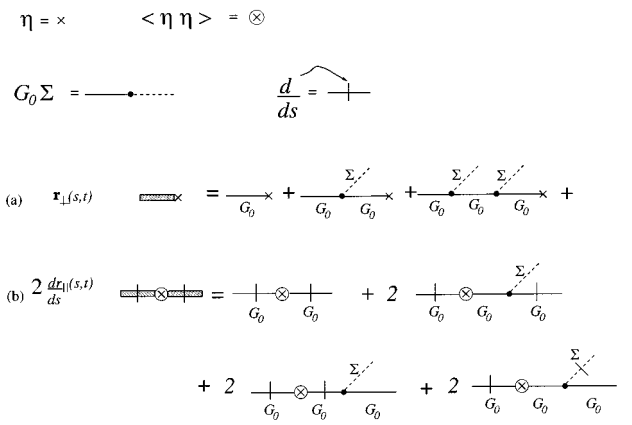

Figure 2. (a) Diagrammatic expansion of $r_\perp$ in Σ (or equivalently τ) to second order in Σ. We have one $\tau - r_\perp$ vertex. The zero-order Green's function $G_0 = (i\omega + H_\perp(k)\alpha k^4)^{-1}$. The noise η is represented by a $\times$. (b) Diagrammatic expansion for $\partial_s r_{||}$ after averaging over the *transverse* noise. We denote an average over the noise by a circle. We have shown only the terms to *linear* order in Σ.

$$R(q,\omega) = \frac{e^{i3\pi/8}}{2k_BT/_p^2}\left(\frac{\alpha\log[a(\omega/\alpha)^{1/4}]}{2\omega}\right)^{3/4}[1 + O(q^4/|\omega|)] \tag{46}$$

Taking the Fourier transform of eq 28 for the longitudinal dynamics

$$-i\omega r_{||}(q,\omega) = \frac{-\log qa}{\zeta_{||}}(iq\tau(q,\omega) + \kappa q^4 r_{||}(q,\omega)) + \eta_{||}(q,\omega) \tag{47}$$

where we have redefined $r_{||}(q,\omega)fr_{||}(q,\omega) \rightarrow \langle r_{||}(q,\omega)\rangle_\perp$. As mentioned above for $q^4 \ll |\omega|/\alpha$, the tension τ dominates the bending contribution, $\kappa q^4 r_{||}$, and therefore substituting eq 44 into eq 47, we obtain in this limit

$$r_{||}(q,\omega) = -G_{||}(q,\omega)\eta_{||}(q,\omega) \tag{48}$$

where

$$G_{||}(q,\omega) = \frac{\zeta_{||}R(q,\omega)}{i\omega\zeta_{||}R(q,\omega) + q^2\log qa} \tag{49}$$

For $q^4 \gg |\omega|/\alpha$, the longitudinal dynamics have the same scaling as the transverse.

The mean square fluctuations of the longitudinal displacements, given by the two-time correlation function defined in eq 17 is given by

$$J_{||}(s,t) = \frac{4k_BT}{\zeta_{||}}\int\int \frac{\mathrm{d}q}{2\pi}\frac{\mathrm{d}\omega}{2\pi}|\log qa|G_{||}(q,\omega)G_{||}(-q,-\omega)\{\cos(qs) - \cos(qs+\omega t)\} \tag{50}$$

The integral above though complicated can be evaluated exactly to give eq 25.

V. Incoherent Dynamic Structure Factor

The incoherent dynamic structure factor was defined in eq 11, section III. Performing the integral over x in eq 15, we obtain

$$S_{\mathrm{inc}}(\mathbf{q}, t) = \exp\left[-\frac{q^2}{4}J_{\perp}(0, t)\right] \times \frac{2\sqrt{\pi}\,\mathrm{erf}(q/2\sqrt{J_{\parallel}(0, t) - J_{\perp}(0, t)})}{q\sqrt{J_{\parallel}(0, t) - J_{\perp}(0, t)}} \quad (51)$$

where $J_{\perp,\parallel}$ were calculated in section IV. We can observe two time regimes in the behavior of the scattering function. The crossover time t_{inc} between the two regimes depends on the scattering wave vector $\mathbf{q}$ and is given by $t_{\mathrm{inc}}(q) \sim ({}^9/_4)^{4/3}\,[(\zeta_{\perp})/(k_{\mathrm{B}}T)]\,(({}^{\prime}\!/_{\mathrm{p}}\pi^4)/(\Gamma^4({}^1/_4)q^8))^{1/3}$.

A. Short Time Expansion. For short times $t \to 0$, we obtain

$$S_{\mathrm{inc}}(\mathbf{q}, t) \simeq 1 - \frac{q^2}{4}\left(\frac{2}{3}\,J_{\perp}(0, t) + \frac{1}{3}\,J_{\parallel}(0, t)\right) \quad (52)$$

We see that both the longitudinal and transverse motion contribute to the scattering function. However at short times, $J_{\perp} \gg J_{\parallel}$ so that the transverse dynamics dominate the scattering. A naive calculation with a static Lagrange multiplier[6,3] would lead to $J_{\perp} = J_{\parallel}$ and thus to a numerical error in the coefficient to decay in the short time behavior.

B. Long Time Expansion. The asymptotic behavior may be calculated for relatively long times. Here we perform a saddle point approximation to the integral in eq 15. The $J_{\perp}$ dominates the integral and we obtain

$$S_{\mathrm{inc}}(\mathbf{q}, t) \sim \frac{3{}^{\prime}\!/_{\mathrm{p}}\pi}{2q^2\Gamma({}^1/_4)({}^{\prime}\!/_{\perp}(t))^3(\log[{}^{\prime}\!/_{\perp}/a])^{3/4}} \times \exp\left[-q^2\frac{2\Gamma({}^1/_8)}{7(2{}^{\prime}\!/_{\mathrm{p}})^5\pi}({}^{\prime}\!/_{\parallel}(t))^7(\log[{}^{\prime}\!/_{\parallel}/a])^{1/2}\right] \quad (53)$$

Thus, the dominant contribution to the scattering function at long time scales is a stretched exponential with stretching exponent ${}^7/_8$. This behavior comes from the longitudinal motion of the filaments; it has not been seen in previous, approximate treatments of the dynamics of stiff polymers. Previous work[6] gives a decay with stretching exponents of ${}^3/_4$. To find this expression, the exact incompressibility constraint has to be imposed locally at all times.

VI. Coherent Dynamic Structure Factor

The coherent dynamic structure factor was defined in eq 18. This scattering function displays three dynamic regimes: (1) *short times* when $q^{-1} \gg {}^{\prime}\!/_{\parallel} \gg {}^{\prime}\!/_{\perp}$, (2) *intermediate times* when ${}^{\prime}\!/_{\parallel} \gg q^{-1} \gg {}^{\prime}\!/_{\perp}$, and (3) *long times* when ${}^{\prime}\!/_{\parallel} \gg {}^{\prime}\!/_{\perp} \gg q^{-1}$. There are two crossover time scales which we call $t^{\mathrm{s}}_{\mathrm{coh}}(q)$ between short and intermediate regimes and $t^{\mathrm{i}}_{\mathrm{coh}}(q)$ between the intermediate and long time behavior given respectively by $t^{\mathrm{s}}_{\mathrm{coh}}$ sim $\zeta_{\parallel}/(2{}^{\prime}\!/_{\mathrm{p}})^5k_{\mathrm{B}}Tq^8$ and $t^{\mathrm{i}}_{\mathrm{coh}}(q) \sim \zeta_{\perp}/{}^{\prime}\!/_{\mathrm{p}}k_{\mathrm{B}}Tq^4$.

A. Short Time Behavior. We find in the limit $t \to 0$

$$S_{\mathrm{coh}}(\mathbf{q}, t) - S^{(0)}(\mathbf{q}) = -q^3t\frac{2k_{\mathrm{B}}T}{3\pi}\left(\frac{2}{\zeta_{\perp}}\log[{}^{\prime}\!/_{\perp}(t)/a] + \frac{1}{\zeta_{\parallel}}\log[{}^{\prime}\!/_{\parallel}(t)/a]\right)\frac{\pi}{2qa} \quad (54)$$

This expression is similar that found in Kroy et al.;[5] however, there are two important differences.

- There is a contribution due to longitudinal motion: Previous calculations were based purely on the transverse fluctuations of the filament, neglecting all longitudinal motion. They find a term similar to just the first contribution on the right of eq 54.
- The authors find an intermediate result which has a weak logarithmic divergence. They argue that this divergence must be cut off by the scattering vector of the radiation. The full calculation presented hear shows that the lengths ${}^{\prime}\!/_{\perp}$ and ${}^{\prime}\!/_{\parallel}$ already cut of the divergence in the calculation.

At first glance, this result may seem surprising since a general result given by Doi and Edwards[1,5] for an arbitrary ensemble of interacting particles seems to prove that the scattering function has a linear dependence in t for small times. Our result is rather in t log t. How is this possible? In fact a close examination of the proof of the "theorem" as stated by Doi and Edwards[1] shows why: The key step in the proof is a (functional) integration by parts of a correlation function. This requires the vanishing of this correlation function at the ultraviolet cutoff ($q \to \infty$). This is true for flexible polymers and is related to the fact that for $qR_{\mathrm{g}} \gg 1$ the static structure function $S^{(0)}(q) \sim q^{-\nu}$ with $\nu < 1$. However for *semiflexible* polymers on length scales less than ${}^{\prime}\!/_{\mathrm{p}}$, $S^{(0)}(q) \sim q^{-1}$ and the correlation function diverges (logarithmically) as $q \to \infty$ making the "theorem" inapplicable for stiff polymers. This was illustrated by the fact that an attempt to use the "theorem" for semiflexible polymers for $q{}^{\prime}\!/_{\mathrm{p}} \gg 1$ gave an integrand which diverged in the limit $q \to \infty$ as pointed out by Kroy and Frey.[5] An attempt was made to rectify the problem[5] by putting an ultraviolet cutoff at $q = 1/a$.

We now sketch the method by which we obtain the above result. For short times, t, $J_i(s, t) \ll 1$, and we can expand the argument of the exponentials $\exp[-q^2(1 - x^2)J_{\perp}(s, t)]$ and $\exp[-q^2x^2J_{\parallel}(s, t)]$; from the expressions for J_i, eqs 22 and 25, we obtain

$$S_{\mathrm{coh}}(\mathbf{q}, t) - S^{(0)}(\mathbf{q}) = -\frac{1}{2N}\int_{-1}^{1}dx\int_{s=0}^{L}\frac{\mathrm{d}s}{a}\int_{s'=0}^{L-s}\frac{\mathrm{d}s'}{a}\,e^{iqxs'} \times \mathrm{e}^{-1/4(q^2(1-x^2)K_{\perp}^{(0)}(s')-q^2x^2K_{\parallel}^{(0)}(s'))} \times \frac{q^2}{4}\{(1 - x^2)J_{\perp}(s', t) + x^2J_{\parallel}(s', t)\} \quad (55)$$

where

$$S^{(0)}(\mathbf{q}) \equiv \frac{1}{2N}\int_{-1}^{1}dx\int_{s}\int_{s'}e^{iqx(s-s')}\mathrm{e}^{-q^2(1-x^2)K_{\perp}^{(0)}(s-s')/4-q^2x^2K_{\parallel}^{(0)}(s-s')/4} \quad (56)$$

is the static structure factor. To calculate the static structure factor, $S^{(0)}(\mathbf{q})$ we perform the integral over x and set the static correlation functions to $K^{(0)} = 0$ as they are of the order of $x^2L/{}^{\prime}\!/_{\mathrm{p}} \to 0$ for $L \ll {}^{\prime}\!/_{\mathrm{p}}$.

$$S^{(0)}(\mathbf{q}) = \frac{1}{2N}\int_0^{Na}\frac{\mathrm{d}s}{a}\int_0^{\infty}\frac{\mathrm{d}s'}{a}\frac{\sin[qs']}{qs'} = \frac{\pi}{2qa} \quad (57)$$

For the dynamic structure factor we can perform the integral over x to obtain

$$S_{\mathrm{coh}}(\mathbf{q}, t) - S^{(0)}(\mathbf{q}) = -\frac{1}{2N}\int_{s=0}^{L}\int_{s'=0}^{L-s}\frac{q^2}{4}\left(\frac{4(\sin qs' - qs'\cos qs')}{q^3s'^3}\right)\times J_{\perp}(s', t) - \frac{1}{2N}\int_{s=0}^{L}\int_{s'=0}^{L-s}\frac{q^2}{4}\times\left(\frac{2(2qs'\cos qs' + (q^2s'^2 - 2)\sin qs')}{q^3s'^3}\right)J_{\parallel}(s', t) \quad (58)$$

First we perform the integral over s'. Before we do that it is convenient to change variables from s' to $\sigma_i \equiv s'A_i(z, t)/a$. Note that $A_i \to \infty$ as $t \to 0$. For *very* short times, $\cos\sigma_i$ dominates the terms like $4(\sin[qs'] - qs'\cos[qs'])/[qs']^3 \sim {}^4/_3$ and

$$S_{\mathrm{coh}}(\mathbf{q}, t) - S^{(0)}(\mathbf{q}) = -\frac{1}{2N}\int_{s=0}^{L}\frac{\mathrm{d}s}{a}\int_{s'=0}^{L-s}\frac{\mathrm{d}s'}{a}\frac{q^2}{4}\left[\frac{4}{3}J_{\perp}(s', t) + \frac{2}{3}J_{\parallel}(s', t)\right] \quad (59)$$

We evaluate the integral over s

$$S_{\mathrm{coh}}(\mathbf{q}, t) - S^{(0)}(\mathbf{q}) = -\frac{4q^2k_{\mathrm{B}}T}{6\pi N}\times\left[\frac{2(\ell_{\perp})^3\log[\ell_{\perp}/a]^{3/4}}{k_{\mathrm{B}}T\ell_{\mathrm{p}}}\int_0^{\infty}\mathrm{d}z\frac{(1 - \mathrm{e}^{-z^4})}{z^4}\times\left(\frac{1 - \cos[A_{\perp}(z\log[\ell_{\perp}/a]^{-1/4}, t)N]}{A_{\perp}^2(z\log[\ell_{\perp}/a]^{-1/4}, t)}\right) + \frac{(\ell_{\parallel})^7\log[\ell_{\parallel}/a]^{1/2}}{k_{\mathrm{B}}T\ell_{\vartheta}^5}\int_0^{\infty}\mathrm{d}z\,\frac{(1 - \mathrm{e}^{-z^8})}{z^8}\times\left(\frac{1 - \cos[A_{\parallel}(z\log[\ell_{\parallel}/a]^{-1/2}, t)N]}{A_{\parallel}^2(z\log[\ell_{\parallel}/a]^{-1/2}, t)}\right)\right] \quad (60)$$

Change variables and expand for t small, but t large enough so that $\ell_{\parallel,\perp}(t) > a$ and we obtain eq 54.

B. Intermediate Time Behavior. The longitudinal fluctuations are propagated faster than the transverse fluctuations so that we always have the inequality $\ell_{\parallel} \gg \ell_{\perp}$. At the crossover time t_{coh}^{s}, the scattering wave vector, q^{-1} becomes comparable to $\ell_{\parallel}$. At this point the longitudinal fluctuations become too weak to contribute significantly to the scattering cross section. The polymer looks uniform in the parallel direction and parallel motion does not couple to density fluctuations. However we are still in a short time regime for transverse fluctuations. In eq 58, the term $2(2qs'\cos qs' + (q^2s'^2 - 2)\sin qs')/q^3s'^3$ dominates the $\cos[\sigma_{\parallel}]$, and performing the integrals over s,σ_i, we obtain

$$S_{\mathrm{coh}}(\mathbf{q}, t) - S_{\mathrm{coh}}^{(0)}(\mathbf{q}) = -q^2t\log[\ell_{\perp}(t)/a]\frac{4k_{\mathrm{B}}T}{3\pi\zeta_{\perp}} - \frac{\Gamma[{}^3/_8]}{5\pi}\left(\frac{\ell_{\parallel}(t)}{2\ell_{\mathrm{p}}}\right)^5\log[\ell_{\parallel}/a]^{-1/2}\frac{\pi}{qa} \quad (61)$$

The second term on the right of eq 61 is much smaller than the first and therefore the longitudinal fluctuations become subdominant and only the transverse motion of the chain contributes to the scattering function.

C. Long Time Behavior. After performing the integrals over s, s' we obtain

$$S_{\mathrm{coh}}(\mathbf{q}, t) - S_{\mathrm{coh}}^{(0)}(\mathbf{q}) = \frac{\pi}{qa}\left(-q^2\ell_{\perp}^2(t)\log[\ell_{\perp}/a]^{3/4}\frac{\Gamma[{}^1/_4]}{3\pi\ell_{\mathrm{p}}} + \frac{\Gamma[{}^3/_4]}{\pi}\frac{\ell_{\perp}(t)}{\ell_{\mathrm{p}}}\log[\ell_{\perp}/a]^{1/4} - \frac{\Gamma[{}^3/_8]}{5\pi}\left(\frac{\ell_{\parallel}(t)}{2\ell_{\mathrm{p}}}\right)^5\log[\ell_{\parallel}/a]^{5/8}\right) \quad (62)$$

The first term is the expected stretched exponential with exponent ${}^3/_4$. However there are important corrections coming from the longitudinal motion which suggest a q-independent renormalization of the ratio $S_{\mathrm{coh}}(\mathbf{q}, t)/S^{(0)}(\mathbf{q})$. This effect should be large enough to be experimentally measurable, above all at small angles.

We now calculate asymptotically the decay of the coherent structure factor, S_{coh} for long times to find

$$S_{\mathrm{coh}}(\mathbf{q}, t) = S_{\mathrm{inc}}(\mathbf{q}, t) + \frac{\pi}{2qa}\exp\left[-q^2\frac{\ell_{\perp}^2(t)\log[\ell_{\perp}/a]^{3/4}\Gamma({}^1/_4)}{6\pi\ell_{\mathrm{p}}}\right] \quad (63)$$

This result (stretched exponential decay with $t^{3/4}$) has been found by several authors[4,5] and has been widely used to interpret quasi-elastic light scattering from semiflexible polymer solutions.[29]

VII. Discussion

A. Experimental Considerations. We have shown that correct calculation of the small time behavior of the coherent and incoherent structure factors requires correct treatment of the longitudinal motion. The coherent structure factor has a particularly rich behavior, with three possible time regimes. At long times, the simplest theories are a good approximation for the coherent structure factor but fail badly for the calculation of the incoherent structure factor which is dominated by the longitudinal motion. We now give simple estimates of typical time scales and to show that these regimes are all experimentally accessible. As examples we take DNA with a persistence length of 50 nm and actin filaments with persistence length 15 μm as a guide for experimentalists pointing out the wave vectors at which experiments could be performed to see our various regimes. All of them should be observable for reasonable values of the decay of the structure factor; i.e., $S(q, t)/S(q, 0) > 0.002$.

Incoherent scattering functions are measured by neutron scattering on isotopically mixed samples. In a spin−echo spectrometer, scattering wave vectors are in the regime $10^{-3}\text{Å}^{-1} < q < 0.1\ \text{Å}^{-1}$. For these wave vectors, DNA has a crossover time scale between the two incoherent scattering regimes, t_{inc}[DNA] in the range $10^{-8}\ \mathrm{s} < t_{\mathrm{inc}}[\mathrm{DNA}] < 10^{-3}\ \mathrm{s}$. Since a typical time-of-flight spin−echo spectrometer has a dynamic range of 10^{-12}−10^{-9} s, the short and long time regimes as well as the crossover between them should be observable.

The coherent scattering function can be measured using both light and neutron scattering techniques. As mentioned in section VI, we predict the existence of three dynamic regimes. In a dynamic light scattering experiment, with a typical temporal range of 1 μs to 1 s, we can estimate the typical wave vectors at which the crossovers between these regimes would be observed

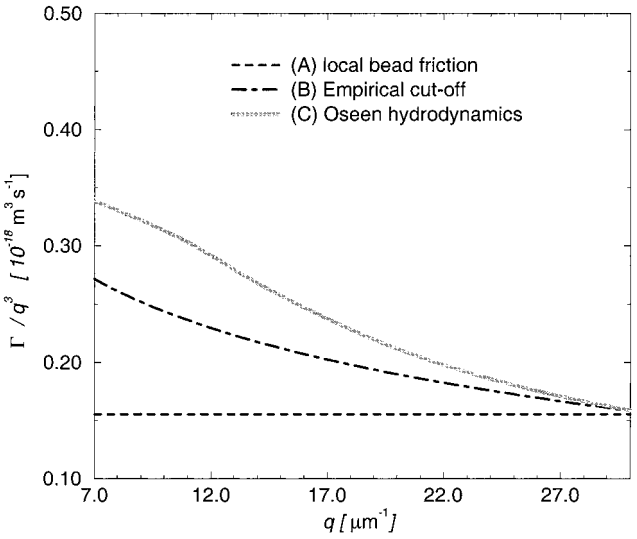

Figure 3. Initial slope Γ/q^3 of $S_{coh}(\mathbf{q}, t)$ for the filamentous phage fd. The three curves correspond to the following approximations: (A) local bead friction given by eq 65; (B) the empirical cut off using the theorem from ref 1 given by eq 66; (C) full Oseen hydrodynamics as presented in this paper given by eq 54.

for the biopolymer actin. For the crossover from the short to intermediate regimes, actin has t^s_{coh}[actin] varying between 10^{-8} s < t^s_{coh}[actin] < 1 s as the wave vector q varies from 1 μm^{-1}(10^{-8} s) > q > 0.1 μm^{-1}(1 s). The crossover time between the long and intermediate regimes, t^i_{coh}[actin] for actin varies between 10^{-5} s < t^i_{coh}[actin] < 0.1 s as the wave vector q varies from 10 μm^{-1}(10^{-5} s) > q > 1 μm^{-1}(0.1 s). Since these *semiflexible* dynamical modes are excited on length scales $L < \ell_p$, we are also restricted to wave vectors $q^{-1} < \ell_p$. If $q^{-1} \gg \ell_p$, we are in the *flexible* polymer regime, and the well-known results for the dynamics of flexible polymers[1] will apply. This is the case for light scattering from DNA. Coherent neutron scattering from DNA is in the right regime to probe the semiflexible dynamics of DNA. As discussed in section IIB, the presence of intrinsic bends due to variations in local base composition could lead to additional contributions to the scattering from DNA. The crossover time, t^s_{coh}[DNA] from short to intermediate time regimes in DNA varies between 10^{-11} s < t^s_{coh}[DNA] < 10^{-3} s as the wave vector q varies from 10^{-2} Å^{-1} (10^{-11} s) > q > 10^{-3} Å^{-1} (10^{-3} s). The intermediate to long time crossover has t^i_{coh}[DNA] varying between 10^{-7}s < t^i_{coh}[DNA] < 10^{-3} s as the wave vector q varies from 10^{-2} Å^{-1}(10^{-7} s) > q > 10^{-3} Å^{-1} (10^{-3} s). Other possible model systems for the study of semiflexible dynamics include polysaccharides such as xanthan.

B. Experiments on Viral Particles. Recently, Augustin[17] performed a detailed comparison between experiments on the fd virus and existing theories of semiflexible polymers. His experimental results were in disagreement with existing theories. Motivated by his measurements, we numerically evaluated the coherent structure function defined in eq 12 using eqs 22 and 25. The virus is known to have a length L = 0.9 μm, diameter a = 6.5 nm, and persistence length ℓ_p = 2.2 μm.[32] He performed his experiments with a minimum sampling time of 1 μs and a maximum time of 1 s. The light scattering experiment was done at wave vectors q ~ 10 μm^{-1} allowing us to calculate the crossover times t^s_{coh}[fd] ~ 10^{-12} s and t^i_{coh}[fd] ~ 10^{-4} s. Their sampling time therefore limits them to the intermediate and long time regimes. The phages are also rather short, and we should compare our dynamic correlation lengths with L. We can calculate the longitudinal and transverse correlation lengths $\ell_\parallel(t = 1\ \mu s) \sim 0.43\ \mu m$ and $\ell_\perp(t = 1\ \mu s) \sim 0.030\ \mu m$, and we see that $\ell_\parallel \sim L$ while $\ell_\perp \ll L$. Our model is valid for t such that $\ell_\perp(t), \ell_\parallel(t) > a$, which is clearly the case in these experiments.

He analyzed the initial slope of the structure function defined by

$$\Gamma(q) = -\frac{d}{dt} \log S_{coh}(\mathbf{q},t)|_{t\to 0} \tag{64}$$

We evaluated the structure function in the time range 5−50 μs and from that calculated the apparent initial slope. In our numerical calculation, we used a polymer hydrodynamic diameter of a = 10 nm (since we are only able to specify the diameter to within a number of order unity) and ℓ_p = 2.2 μm. We used as the viscosity of water at room temperature $\zeta_s = 0.891 \times 10^{-3}$ Pa s. Since we evaluate the integrals in eq 12 numerically, we make no approximations and our results are limited only by the accuracy of the integration algorithm. We used a as the *natural* length scale for discretization in the s integrals. Using the same wave vector range 5 < q < 30 μm^{-1} as Augustin,[17] we compare our results for the initial slope, Γ using the full hydrodynamics to that obtained using a local bead model, i.e.

$$\Gamma(q) = \frac{2k_BT}{6\pi^2\zeta_s} q^3 \tag{65}$$

We also compared our results with the initial slope calculated by Kroy et al.[5] using the result for the initial slope of the scattering function from[1] with an empirical cutoff at $1/a$

$$\Gamma(q) = \frac{k_BT}{6\pi^2\zeta_s} q^3 (^5/_6 - \ln qa) \tag{66}$$

The results for the three calculations are plotted in Figure 3. We observe that the value of Γ calculated from local friction or the empirical cutoff[5] is underestimated as $q \to 0$. This is in agreement with the experiment.

The scattering vectors used in this experiment together with the shortness of the virus particles prevented the study of the true short time regime. Such studies should be possible however with low angle light scattering from actin solutions, where strong enhancement of Γ/q^3 should be found in addition to that presented in Figure 3 for viral particles.

C. Other Experiments. Dynamic light scattering experiments on Desmin filaments[30] and Fibrin networks[31] have also analyzed the short time behavior and found big deviations from the local bead models. They analyzed their data using the empirical cutoff theory.[5] Our theory would also predict similar behavior without the need for an empirical cutoff. It would be interesting to reanalyze their results with our theory.

Acknowledgment. We would like to thank A. Ajdari, R. Everaers, and K. Kroy for many helpful discussions and encouragement. The financial support of the European Union under a Marie Curie research grant,

No. FMBICT972699, and the Royal Society is gratefully acknowledged (T.B.L.).

References and Notes

(1) Doi, M.; Edwards, S. F. *The Theory of Polymer Dynamics*; Clarendon Press: Oxford, U.K., 1986.
(2) de Gennes, P. G. *Scaling concepts in polymer physics*; Cornell University press: Ithaca, NY, 1979.
(3) Harris, R. A.; Hearst, J. E. *J. Chem. Phys.* **1996**, *44*, 2525.
(4) Farge, E.; Maggs, A. C. *Macromolecules* **1993**, *26*, 5041.
(5) Kroy, K.; Frey, E. *Phys. Rev. E*, **1997**, *55*, 3092. Kroy, K.; Frey, E. In *Scattering in Polymeric and Colloidal Systems*; Brown, W., Mortensen, K., Eds.; Gordon and Breach: London, 2000.
(6) Harnau, L.; Winkler, R. G.; Reineker, P. *J. Chem. Phys.* **1995**, *102*, 7750. Harnau, L.; Winkler, R. G.; Reineker, P. *J. Chem. Phys.* **1996**, *104*, 6355. Harnau, L.; Winkler, R. G.; Reineker, P. *J. Chem. Phys.* **1997**, *106*, 2469.
(7) Bawendi, M.; Freed, K. *J. Chem. Phys.* **1985**, *83*, 2491.
(8) Schurr, J. M.; Fujimoto, B. S. *Biopolymers* **2000**, *54*, 561.
(9) Wilhelm, J.; Frey, E. *Phys. Rev. Lett.* **1996**, *77*, 2581.
(10) Schmidt, C. F.; Bärmann, M.; Isenberg, G.; Sackmann, E. *Macromolecules* **1989**, *22*, 3638.
(11) Schmidt, M.; Stockmayer, W. H. *Macromolecules* **1984**, *17*, 509.
(12) Maeda, T.; Fujime, S. *Macromolecules* **1984**, *17*, 3281.
(13) Aragón, S. R.; Pecora, R. *Macromolecules* **1985**, *18*, 1868.
(14) Gittes, F.; MacKintosh, F. *Phys. Rev. E* **1998**, *58*, R1241.
(15) Everaers, R.; Jülicher, F.; Ajdari, A.; Maggs, A. C. *Phys. Rev. Lett.* **1999**, *82*, 3717.
(16) Ahlrichs, P. Doktorarbeit, Universität Mainz, 2000. http://www.mpip-mainz.mpg.de/www/theory/phd_work/phd-ahlrichs.ps.gz.
(17) Augustin, A. Diplomarbeit, Technische Universität München, 1999. http://zk.bwh.harvard.edu/people/alumni/thesis.pdf.
(18) Kratky, O.; Porod, G. *Recl. Trav. Chim. Pays-Bas* **1949**, *68*, 1106.
(19) Seifert, U.; Wintz, W.; Nelson, P. *Phys. Rev. Lett.* **1996**, *77*, 5389.
(20) Chaikin, P.; Lubensky, T. *Principles of Condensed Matter Physics*, C.U.P.: Cambridge, U.K., 1995.
(21) Fuller, F. B. *Proc. Natl. Acad. Sci. U.S.A.* **1971**, *68*, 815. Fuller, F. B. *Proc. Natl. Acad. Sci. U.S.A.* **1975**, *75*, 3557.
(22) Levinthal, C.; Crane, H. R. *Proc. Natl. Acad. Sci. U.S.A.* **1956**, *42*, 436.
(23) Nelson, P. *Proc. Natl. Acad. Sci. U.S.A.* **1999**, *96*, 14342.
(24) Maggs, A. C. *cond-mat/9712053*, http://arXiv.org/abs/cond-mat/9712053.
(25) Maggs, A. C. *Phys. Rev. Lett.* **2000**, *85*, 5472.
(26) Schurr, J. M.; Fujimoto, B. S.; Reese, A.; Robinson, B. H.; Allison, S. A. *J. Chem. Phys.* **1997**, *106*, 815.
(27) Higgins, J. S.; Benoit, H. C. *Polymers and Neutron Scattering*; Clarendon Press: Oxford, U.K., 1994.
(28) Dichtl, M. A.; Sackmann, E. *New J. Phys.* **1999**, *1*, 18.
(29) Götter, R.; Kroy, K.; Frey, E.; Bärmann, M.; Sackmann, E. *Macromolecules* **1996**, *29*, 30.
(30) Hohenadl, M.; Storz, T.; Kirpal, H.; Kroy, K.; Merkel, R. *Biophys. J.* **1999**, *77*, 2199.
(31) Arcovito, G.; Bassi, F. A.; De Spirito, M.; Di Stasio, E.; Sabetta, M. *Biophys. Chem.* **1997**, *67*, 287.
(32) Song, L.; Kim, U. S.; Wilcoxon, J.; Schurr, J. M. *Biopolymers* **1991**, *31*, 547.

MA001468P